

# QhX: A Python package for periodicity detection in red noise

Andjelka B. Kovačević<sup>1\*</sup>, Dragana Ilić<sup>1</sup>, Momčilo Tošić<sup>1\*</sup>, Marina Pavlović<sup>2</sup>, Aman Raju<sup>3</sup>, Mladen Nikolić<sup>1</sup>, Saša Simić<sup>4</sup>, Iva Čvorović-Hajdinjak<sup>1</sup>, and Luka Č. Popović<sup>5</sup>

1 University of Belgrade - Faculty of Mathematics, Studentski trg 16, Belgrade, Serbia 2 Rubin Observatory Project Office, 950 N. Cherry Ave., Tucson, AZ 85719, USA 3 DARK, Niels Bohr Institute, University of Copenhagen, Jagtvej 155, Copenhagen N, 2200, Denmark 4 Faculty of sciences, University of Kragujevac, Radoja Domanovića 12, Serbia 5 Astronomical Observatory, Belgrade, Volgina 7, 11000 Belgrade, Serbia ¶ Corresponding author \* These authors contributed equally.

DOI: [10.21105/joss.08163](https://doi.org/10.21105/joss.08163)

## Software

- [Review](#) ↗
- [Repository](#) ↗
- [Archive](#) ↗

---

Editor: [Ivelina Momcheva](#) ↗ ⓘ

Reviewers:

- [@sgeorge91](#)
- [@Zstone19](#)

Submitted: 18 November 2024

Published: 01 January 2026

## License

Authors of papers retain copyright and release the work under a Creative Commons Attribution 4.0 International License ([CC BY 4.0](#)).

## Summary

QhX is a Python package for detecting periodicity in red noise time series, developed as an in-kind contribution to the Vera C. Rubin Observatory Legacy Survey of Space and Time (LSST, [Ivezic et al., 2019](#)). Traditional Fourier-based methods often struggle with red noise, which is common in quasar light curves and other accreting objects. QhX addresses these challenges with its core 2-dimensional (2D) hybrid method ([Kovačević et al., 2018](#)). Input data are mapped into a time-period plane via wavelet transforms, which are (auto)correlated to produce a correlation density map in a “period-period” plane. Statistical vetting incorporates significance, upper and lower error bounds, and the novel intersection over union (IoU) metric to evaluate the proximity and overlap of detected periods across bands and objects. In addition to a vetted numerical catalog, QhX dynamically visualizes periodicity across photometric bands and objects.

## Statement of need

Periodic variability spans a range of astronomical objects, from asteroids to quasars. Identifying meaningful signals is complicated by red noise (see, for example, Figure 1 in [Gaia Collaboration et al., 2019](#); [Kasliwal et al., 2015](#); [Kovačević, Radović, et al., 2022](#)), which exhibits fractal-like patterns across time scales ([Belete et al., 2018](#); [Vio et al., 1991](#)). Non-stationary signals and unfavorable sampling ([Brandt et al., 2018](#); [D’Orazio & Charisi, 2023](#)) further obscure coherent patterns. Traditional time-frequency methods are often ineffective with such complex signals due to the Fourier–Gabor uncertainty limit ([Gabor, 1947](#)), highlighting the need for nonlinear approaches ([Abry et al., 1995](#); [Cohen, 1995](#)).

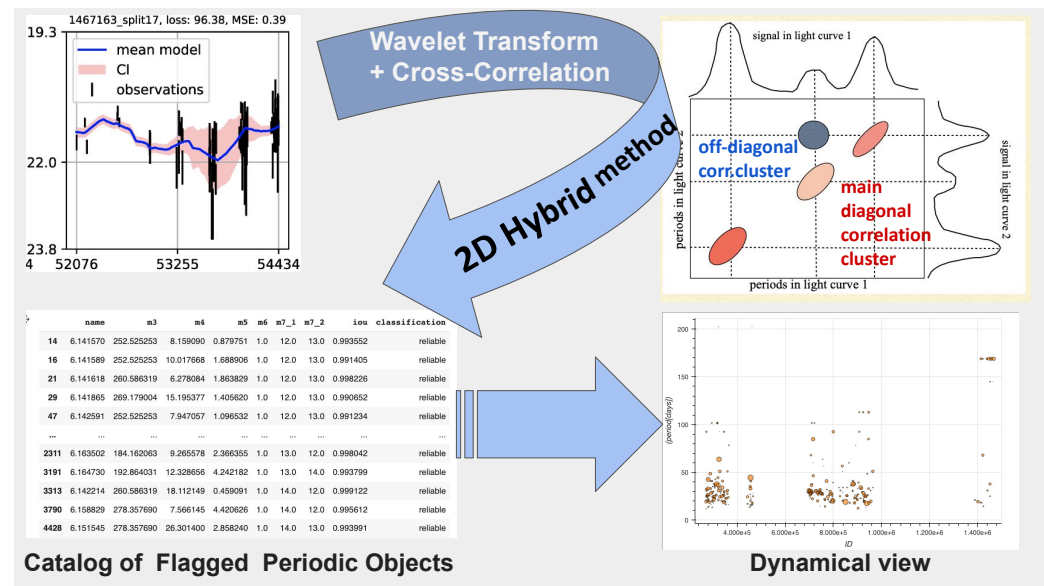


**Figure 1:** The left panel shows a one-dimensional (1D) light curve of observational data (black error bars) and a model (blue line). QhX transforms the time-series data into the time-frequency domain and cross-correlates wavelet matrices to produce a 2D period-period correlation map (right). Clusters in this map indicate periodic signals. After map integration, statistical vetting generates a numerical catalog of flagged periodic objects (bottom left) and a dynamic view of detected periods across objects and bands (bottom right).

QhX provides features specifically designed to address these challenges. The first feature is its core 2D hybrid method (see Figure 1), which is detailed in (Kovačević et al., 2018) and inspired by 2D correlation spectroscopy (Kovačević, 2024; Noda, 2018). By applying wavelet transforms, QhX maps time-series data into the time-frequency domain and (auto)correlates it, generating a period-period correlation density that enhances signal detection. Secondly, QhX introduces an IoU metric, combined with standard statistical measures (significance, upper and lower error bounds), to evaluate the overlap of detected periods across bands and objects. Each period is represented as the center of an “IoU ball,” with its radius reflecting relative error, calculated as the mean of the upper and lower error bounds and analogous to a circular aperture in photometry (Saxena et al., 2024). Finally, QhX enhances traditional analysis by generating numerical and interactive visual catalogs that rank periodicity candidates by reliability. These interactive catalogs enable detailed inspection of signal consistency and offer greater interpretability than traditional static plots.

## QhX structure

QhX (version 0.2.0) is an open-source package optimized for gappy quasar light curves, though it can be adapted to other datasets. It supports both dynamic and fixed modes, with parallel processing capabilities for large-scale data. The modular design facilitates rapid experimentation by enabling easy swapping or modification of functions (see Figure 2), addressing diverse research needs. For fixed-only workflows, specialized functions such as `data_manager` offer minimal overhead and optimal performance, while `data_manager_dynamical` supports both dynamic and fixed configurations to handle more complex scenarios involving dynamic filters.

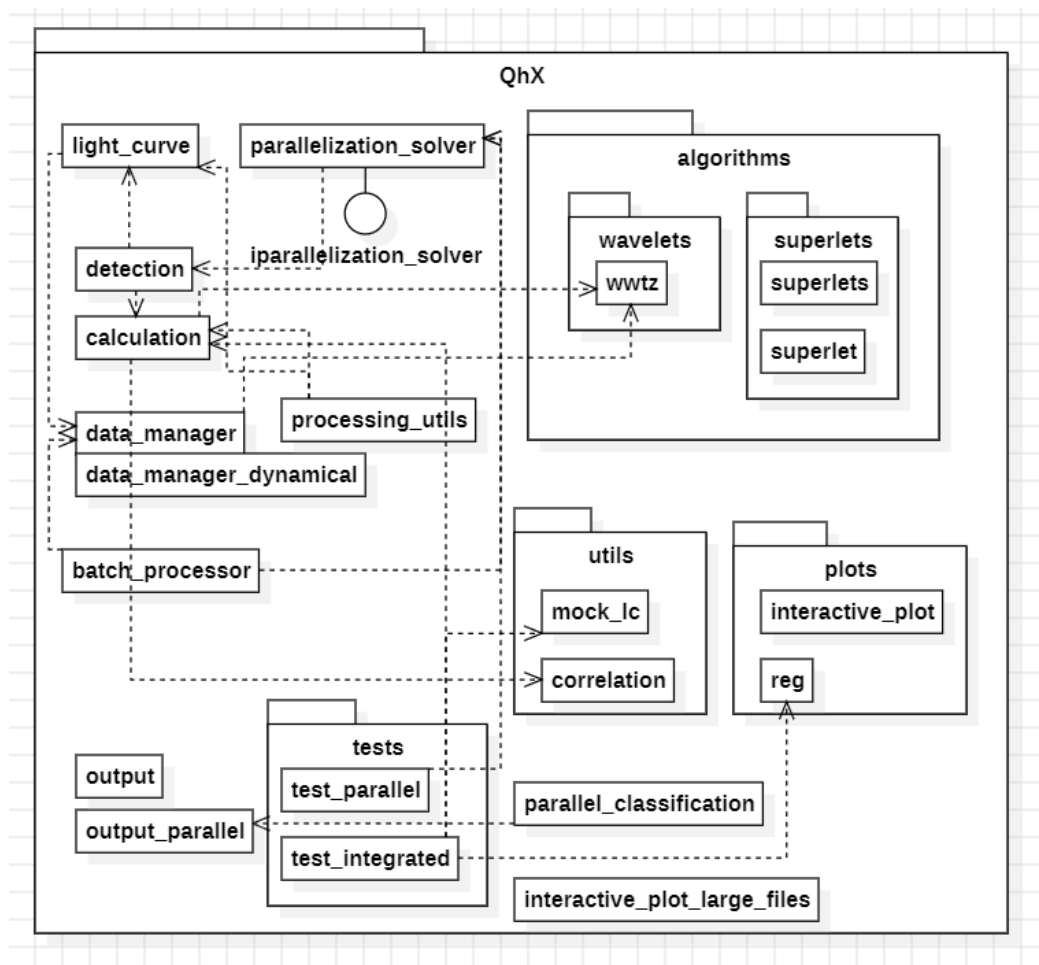


Figure 2: Schematic representation of the QhX package architecture.

The package is organized as follows:

1. Core:

- The algorithms module provides essential signal processing techniques, including the weighted wavelet Z-transform (wwtz) and prototype superlet transforms.
- The correlation function within the utils module supports the 2D hybrid method by converting light curve data into wavelet matrices and creating correlation density via (auto)correlation.

2. Signal detection and validation:

- The detection module identifies candidate periodic signals and assesses their validity using statistical measures such as significance and upper and lower error (Johnson et al., 2019). The IoU metric identifies overlapping periods across bands and objects. To our knowledge, this is the first application of the IoU metric to quantify the overlap between detected and reference periods in astronomical time-series analysis.
- Statistical vetting categorizes detected periods for each object and band as reliable, medium, or poor.

3. Data management:

- QhX takes time-series data as input in a simple tabular format containing time, flux (or magnitude), and associated uncertainties. Examples in the documentation illustrate how to map data from other commonly used formats into this structure.
- The data\_manager and data\_manager\_dynamical modules manage data flow, data

loading, outlier removal, and format compatibility.

- The batch\_processor and parallelization\_solver modules optimize task distribution across multiple processors.

#### 4. Visualization and output:

- The plots module includes tools for creating interactive visualizations. For example, interactive\_plot allows one to explore detected periodicities across bands and objects. For large datasets, interactive\_plot\_large\_files enables in-depth inspection of signal consistency.
- The output and output\_parallel modules handle result storage and support both single-threaded and parallelized workflows.

#### 5. Testing:

- The tests module, containing test\_parallel and test\_integrated, validates the functionality across various processing setups.

## Representative Applications

QhX has been benchmarked with respect to widely used periodicity detection software libraries across multiple domains.

Applications of QhX to quasars demonstrate that its period estimates and significance assessments closely align with those obtained from established methods such as Lomb-Scargle, Generalized Extreme Value (GEV) analyses, and Bayesian evaluations. In Fatović et al. (2023), applying QhX to SDSS J2320+0024 yielded a period of  $278.36^{+57.34}_{-25.21}$  days, with a significance level greater than 99% as measured via the shuffling method and 90% as measured via the GEV approach. A Lomb-Scargle periodogram applied to the same dataset produced a consistent period of 278 days at the same significance level. In Kovačević et al. (2019), QhX detected periods of  $1972 \pm 254$  days (observed light curve) and  $1873 \pm 250$  days (modeled light curve) for PG 1302–102, both within  $1\sigma$  of the  $1884 \pm 88$  day period reported by Graham et al. (2015) using generalized Lomb-Scargle, wavelet, and autocorrelation methods. A Bayesian reanalysis by Zhu & Thrane (2020) on an extended dataset for PG 1302–102 yielded a comparable quasi-period of 5.6 years, which was interpreted as quasiperiodic oscillations. In the case of Mrk 231 (Kovačević, Yi, et al., 2020), the 2D hybrid method identified a characteristic period of 403 days with a significance greater than 99.7%, in agreement with a Lomb-Scargle periodogram result of 413 days at a significance above 95%. The slightly larger uncertainty in the QhX-derived period reflects the temporal variation of the periodicity, while the average oscillation power is comparable between the two methods. This method has also been validated in the context of damped oscillations in the changing-look quasar NGC 3516 (Kovačević, Popović, et al., 2020), where experimental results demonstrated robustness against the combined effects of red noise and complex time-series structure.

Beyond astrophysical applications, QhX has been applied to very low frequency (VLF) signal analysis for pre- and post-earthquake intervals (Kovačević, Nina, et al., 2022). In the no-earthquake scenario (same date one year earlier), the topology of the QhX 2D hybrid maps exhibited distinct correlation cluster patterns compared to the earthquake-day records. Most intervals had detected periods below 111 seconds, and a 140-second signal was detected in the -2-hour segment. This signal closely matched the 147-second signal detected during the earthquake event. Comparison with Fast Fourier Transform (FFT) results (Nina et al., 2020) showed strong agreement before the earthquake for periods below 1.5 minutes, and convergence of both methods to similar values in subsequent intervals. Post-earthquake periods obtained with QhX were also consistent with the  $< 10$  seconds to few-hundred-second range reported in (Ohya et al., 2018).

QhX is [an LSST directable software in-kind contribution](#).

## Acknowledgements

Funding was provided by the University of Belgrade - Faculty of Mathematics (the contract 451-03-66/2024-03/200104), Faculty of Sciences University of Kragujevac (451-03-65/2024-03/200122), and Astronomical Observatory Belgrade (contract 451-03-66/2024-03/200002), through grants by the Ministry of Education, Science, and Technological Development of the Republic of Serbia. QhX makes extensive use of several open-source scientific Python libraries. Core numerical operations and statistical routines rely on NumPy ([Harris et al., 2020](#)) and SciPy ([Virtanen et al., 2020](#)). The weighted wavelet Z-transform calculations are performed using the libwwz library ([ISLA-UH, 2024](#)). Interactive visualization and exploratory analysis are implemented using HoloViews ([Rudiger et al., 2021](#)) with Bokeh ([Bokeh Development Team, 2018](#)) as the plotting backend. We gratefully acknowledge the developers and maintainers of these packages.

## References

- Abry, P., Gonçalvès, P., & Flandrin, P. (1995). *Wavelets, spectrum analysis and 1/f processes* (A. Antoniadi & G. Oppenheim, Eds.; pp. 15–29). Springer New York. [https://doi.org/10.1007/978-1-4612-2544-7\\_2](https://doi.org/10.1007/978-1-4612-2544-7_2)
- Belete, A. B., Bravo, J. P., Canto Martins, B. L., Leão, I. C., De Araujo, J. M., & De Medeiros, J. R. (2018). Multifractality signatures in quasars time series - I. 3C 273. *Monthly Notices of the Royal Astronomical Society*, 478(3), 3976–3986. <https://doi.org/10.1093/mnras/sty1316>
- Bokeh Development Team. (2018). *Bokeh: Python library for interactive visualization*. <https://bokeh.pydata.org/en/latest/>.
- Brandt, W. N., Ni, Q., Yang, G., Anderson, S. F., Assef, R. J., Barth, A. J., Bauer, F. E., Bongiorno, A., Chen, C.-T., De Cicco, D., Gezari, S., Grier, C. J., Hall, P. B., Hoenig, S. F., Lacy, M., Li, J., Luo, B., Paolillo, M., Peterson, B. M., ... Yu, Z. (2018). Active galaxy science in the LSST deep-drilling fields: Footprints, cadence requirements, and total-depth requirements. *arXiv e-Prints*, arXiv:1811.06542. <https://doi.org/10.48550/arXiv.1811.06542>
- Cohen, L. (1995). *Time-frequency analysis*. Prentice Hall PTR. ISBN: 9780135945322
- D'Orazio, D. J., & Charisi, M. (2023). Observational signatures of supermassive black hole binaries. *arXiv e-Prints*, arXiv:2310.16896. <https://doi.org/10.48550/arXiv.2310.16896>
- Fatović, M., Palaversa, L., Tisanić, K., Thanjavur, K., Ivezić, Ž., Kovačević, A. B., Ilić, D., & Č. Popović, L. (2023). Detecting long-period variability in the SDSS Stripe 82 standards catalog. *The Astronomical Journal*, 165(4), 138. <https://doi.org/10.3847/1538-3881/acb596>
- Gabor, D. (1947). Acoustical quanta and the theory of hearing. *Nature*, 159(4044), 591–594. <https://doi.org/10.1038/159591a0>
- Gaia Collaboration, Eyer, L., Rimoldini, L., Audard, M., Anderson, R. I., Nienartowicz, K., Glass, F., Marchal, O., Grenon, M., Mowlavi, N., Holl, B., Clementini, G., Aerts, C., Mazeh, T., Evans, D. W., Szabados, L., Brown, A. G. A., Vallenari, A., Prusti, T., ... Zwitter, T. (2019). Gaia Data Release 2. Variable stars in the colour-absolute magnitude diagram. *Astronomy & Astrophysics*, 623, A110. <https://doi.org/10.1051/0004-6361/201833304>
- Graham, M. J., Djorgovski, S. G., Stern, D., Glikman, E., Drake, A. J., Mahabal, A. A., Donalek, C., Larson, S., & Christensen, E. (2015). A possible close supermassive black-hole binary in a quasar with optical periodicity. *Nature*, 518(7537), 74–76. <https://doi.org/10.1038/nature14143>

- Harris, C. R., Millman, K. J., Walt, S. J. van der, & others. (2020). Array programming with NumPy. *Nature*, 585, 357–362. <https://doi.org/10.1038/s41586-020-2649-2>
- ISLA-UH. (2024). *libwwz: A Python library for the weighted wavelet Z-transform*. <https://github.com/ISLA-UH/libwwz>.
- Ivezić, Ž., Kahn, S. M., Tyson, J. A., Abel, B., Acosta, E., Allsman, R., Alonso, D., AlSayyad, Y., Anderson, S. F., Andrew, J., Angel, J. R. P., Angeli, G. Z., Ansari, R., Antilogus, P., Araujo, C., Armstrong, R., Arndt, K. T., Astier, P., Aubourg, É., ... Zhan, H. (2019). LSST: From science drivers to reference design and anticipated data products. *The Astrophysical Journal*, 873(2), 111. <https://doi.org/10.3847/1538-4357/ab042c>
- Johnson, M. A. C., Gandhi, P., Chapman, A. P., Moreau, L., Charles, P. A., Clarkson, W. I., & Hill, A. B. (2019). Prospecting for periods with LSST - low-mass X-ray binaries as a test case. *Monthly Notices of the Royal Astronomical Society*, 484(1), 19–30. <https://doi.org/10.1093/mnras/sty3466>
- Kasliwal, V. P., Vogeley, M. S., & Richards, G. T. (2015). Are the variability properties of the Kepler AGN light curves consistent with a damped random walk? *Monthly Notices of the Royal Astronomical Society*, 451(4), 4328–4345. <https://doi.org/10.1093/mnras/stv1230>
- Kovačević, A. B. (2024). Two-dimensional (2D) hybrid method: Expanding 2D correlation spectroscopy (2D-COS) for time series analysis. *Applied Spectroscopy*, 0(0), 00037028241241308. <https://doi.org/10.1177/00037028241241308>
- Kovačević, A. B., Nina, A., Popović, L. Č., & Radovanović, M. (2022). Two-dimensional correlation analysis of periodicity in noisy series: Case of VLF signal amplitude variations in the time vicinity of an earthquake. *Mathematics*, 10(22). <https://doi.org/10.3390/math10224278>
- Kovačević, A. B., Pérez-Hernández, E., Popović, L. Č., Shapovalova, A. I., Kollatschny, W., & Ilić, D. (2018). Oscillatory patterns in the light curves of five long-term monitored type 1 active galactic nuclei. *Monthly Notices of the Royal Astronomical Society*, 475(2), 2051–2066. <https://doi.org/10.1093/mnras/stx3137>
- Kovačević, A. B., Popović, L. Č., & Ilić, D. (2020). Two-dimensional correlation analysis of periodicity in active galactic nuclei time series. *Open Astronomy*, 29(1), 51–55. <https://doi.org/10.1515/astro-2020-0007>
- Kovačević, A. B., Popović, L. Č., Simić, S., & Ilić, D. (2019). The optical variability of supermassive black hole binary candidate PG 1302-102: Periodicity and perturbation in the light curve. *The Astrophysical Journal*, 871(1), 32. <https://doi.org/10.3847/1538-4357/aaf731>
- Kovačević, A. B., Radović, V., Ilić, D., Popović, L. Č., Assef, R. J., Sánchez-Sáez, P., Nikutta, R., Raiteri, C. M., Yoon, I., Homayouni, Y., Li, Y.-R., Caplar, N., Czerny, B., Panda, S., Ricci, C., Jankov, I., Landt, H., Wolf, C., Kovačević-Đođčinović, J., ... Marčeta-Mandić, S. (2022). The LSST era of supermassive black hole accretion disk reverberation mapping. *The Astrophysical Journal Supplement Series*, 262(2), 49. <https://doi.org/10.3847/1538-4365/ac88ce>
- Kovačević, A. B., Yi, T., Dai, X., Yang, X., Čvorović-Hajdinjak, I., & Popović, L. Č. (2020). Confirmed short periodic variability of subparsec supermassive binary black hole candidate Mrk 231. *Monthly Notices of the Royal Astronomical Society*, 494(3), 4069–4076. <https://doi.org/10.1093/mnras/staa737>
- Nina, A., Pulinets, S., Biagi, P. F., Nico, G., Mitrović, S. T., Radovanović, M., & Popović, L. Č. (2020). Variation in natural short-period ionospheric noise, and acoustic and gravity waves revealed by the amplitude analysis of a VLF radio signal on the occasion of the Kraljevo earthquake (Mw = 5.4). *Science of the Total Environment*, 710, 136406. <https://doi.org/10.1016/j.scitotenv.2019.136406>

- Noda, I. (2018). Chapter 2 - advances in two-dimensional correlation spectroscopy (2DCOS). In J. Laane (Ed.), *Frontiers and advances in molecular spectroscopy* (pp. 47–75). Elsevier. <https://doi.org/10.1016/B978-0-12-811220-5.00002-2>
- Ohya, H., Tsuchiya, F., Takishita, Y., Shinagawa, H., Nozaki, K., & Shiokawa, K. (2018). Periodic oscillations in the D region ionosphere after the 2011 Tohoku earthquake using LF standard radio waves. *Journal of Geophysical Research: Space Physics*, 123(6), 5261–5270. <https://doi.org/10.1029/2018JA025289>
- Rudiger, P., Stevens, J.-L., Bednar, J. A., Nijholt, B., Mease, J., Andrew, B. C., Radelhoff, A., Tenner, V., maxalbert, Kaiser, M., ea42gh, Samuels, J., stonebig, Pevey, K., LB, Tolmie, A., Stephan, D., Hoxbro, M., & others. (2021). *HoloViz/HoloViews: Version 1.14.2* (Version v1.14.2). Zenodo. <https://doi.org/10.5281/zenodo.4581995>
- Saxena, A., Salvato, M., Roster, W., Shirley, R., Buchner, J., Wolf, J., Kohl, C., Starck, H., Dwelly, T., Comparat, J., & al., et. (2024). CIRCLEZ : Reliable photometric redshifts for active galactic nuclei computed solely using photometry from Legacy Survey Imaging for DESI. *Astronomy & Astrophysics*, 690, A365. <https://doi.org/10.1051/0004-6361/202450886>
- Vio, R., Cristiani, S., Lessi, O., & Salvadori, L. (1991). 3C 345: Is the variability of quasars nonlinear? *The Astrophysical Journal*, 380, 351. <https://doi.org/10.1086/170594>
- Virtanen, P., Gommers, R., Oliphant, T. E., & others. (2020). SciPy 1.0: Fundamental algorithms for scientific computing in Python. *Nature Methods*, 17, 261–272. <https://doi.org/10.1038/s41592-019-0686-2>
- Zhu, X.-J., & Thrane, E. (2020). Toward the unambiguous identification of supermassive binary black holes through Bayesian inference. *The Astrophysical Journal*, 900(2), 117. <https://doi.org/10.3847/1538-4357/abac5a>